Imaging of the Surface of Living Cells by Low-Force Contact-Mode Atomic Force Microscopy

Christian Le Grimellec,* Eric Lesniewska,# Marie-Cécile Giocondi,* Eric Finot,# Véronique Vié,* and Jean-Pierre Goudonnet#

*Centre de Biochimie Structurale, INSERM U414, I.U.R.C., 34093 Montpellier Cedex 05, and #Laboratoire de Physique, CNRS-URA 5027, UFR Sciences et Techniques, BP 400, 21011 Dijon Cedex, France

ABSTRACT The membrane surface of living CV-1 kidney cells in culture was imaged by contact-mode atomic force microscopy using scanning forces in the piconewton range. A simple procedure was developed for imaging of the cell surface with forces as low as 20–50 pN, i.e., two orders of magnitude below those commonly used for cell imaging. Under these conditions, the indentation of the cells by the tip could be reduced to less than l0 nm, even at the cell center, which gave access to the topographic image of the cell surface. This surface appeared heterogeneous with very few villosities and revealed, only in distinct areas, the submembrane cytoskeleton. At intermediate magnifications, corresponding to 20–5 μm scan sizes, the surface topography likely reflected the organization of submembrane and intracellular structures on which the plasma membrane lay. By decreasing the scan size, a lateral resolution better than 20 nm was routinely obtained for the cell surface, and a lateral resolution better than 10 nm was obtained occasionally. The cell surface appeared granular, with packed particles, likely corresponding to proteins or protein-lipid complexes, between ~5 and 30 nm *xy* size.

INTRODUCTION

Imaging of cell surfaces was early considered an important biological application of scanning probe microscopy (Ruppersberg et al., 1989; Ito et al., 1991) and, more particularly, of the atomic force microscope (AFM) (Butt et al., 1990; Häberle et al., 1991; Henderson et al., 1992; Hörber et al., 1992; Radmacher et al., 1992). Whereas examination by the AFM of two-dimensional arrays of proteins can reveal subnanometer details (Müller et al., 1995b; Shao et al., 1996), the best resolution that can be achieved at the surface of cells, either fixed or living, is generally considered to be in the range of 50–500 nm (Fritz et al., 1994; Radmacher, 1997). Among the identified factors that can affect the quality of imaging, such as the strength of the cell adherence to its support, the cell type, the complexity of the topography, and composition of the surface (Henderson, 1994; Hoh and Schoenenberger, 1994; Le Grimellec et al., 1994), a key role was early attributed to the force applied during scanning (Henderson et al., 1992). Thus deformation of the cell surface under the AFM tip due to the generally high scanning forces, between 1 and 30 nN, considered to be necessary for stable imaging (Putman et al., 1994; Hoh and Schoenenberger, 1994; Haydon et al., 1996; Radmacher et al., 1996; Schaus and Henderson, 1997), is likely to limit the lateral resolution obtained on intact cells (Weisenhorn et al., 1993; Radmacher et al., 1995) and to give images whose contrast markedly depends on the rigidity of submembrane stuctures (Henderson et al., 1992; Hoh and Schoenenberger, 1994).

These problems in cell imaging have motivated us to develop a procedure that allows us to image, in the contact mode, the surface of intact cells at much lower forces. The recent finding that single loops connecting bacteriorhodopsin transmembrane helices are in an extended configuration at forces below 200 pN and compressed at forces above this threshold (Müller et al., 1995a) gave us an idea of the range of forces that should be used for cell imaging.

In this paper we describe a simple procedure that makes it possible to image, in the contact mode, living cells with forces as low as 20–50 pN. In this range of forces, indentation of the surface by the tip was generally less than 10 nm, giving access to the cell surface topography. The lateral resolution obtained was routinely better than 20 nm and, occasionally, better than 10 nm.

MATERIALS AND METHODS

Materials

Culture media were from Gibco (Paisley, Scotland). All reagents were of analytical grade.

Cell culture

CV-1 cells (African green monkey kidney cells) were grown at 37°C, in Dulbecco's modified Eagle's medium supplemented with 10% fetal calf serum, 2 mM glutamine, 100 IU/ml penicillin, and 100 μg/ml streptomycin, in a 5% CO_2/95% air atmosphere (Le Grimellec et al., 1997). Cells were grown directly on uncoated glass coverslips (14-mm diameter or 22 × 50 mm) and examined in the subconfluent state. Before examination in the "fluid cell" (Digital Instruments, Santa Barbara, CA) of the AFM, living cells were washed three times with phosphate-buffered saline (125 mM NaCl, 20 mM Na_2HPO_4, 5 mM NaH_2PO_4, 5 mM KCl, pH 7.4)

Received for publication 11 December 1997 and in final form 3 May 1998.

Address reprint requests to Dr. C. Le Grimellec, C.B.S., INSERM U414 I.U.R.C., 75 rue de la Cardonille, 34093 Montpellier Cedex 05, France. Tel.: 33-467-41-59-12; Fax: 33-467-41-59-12; E-mail: clg@iurc1.iurc.montp.inserm.fr.

0006-3495/98/08/695/09 $2.00

containing 0.5 mM $CaCl_2$ and 2 mM glutamine, before imaging in the same buffer (Le Grimellec et al., 1994) at room temperature.

Atomic force microscopy

A multimode Nanoscope III AFM or a Bioscope (Digital Instruments) was used for the experiments. When the Nanoscope III was used, samples were glued to magnetic stainless punches and mounted in the fluid cell without using the O ring. The rectangular coverslips were mounted directly on the stage of the inverted microscope (Zeiss) of the Bioscope. V-shaped silicon nitride cantilevers, with a nominal spring constant of 0.01 N/m (Park Scientific Instruments, Sunnyvale, CA), were used in most of the experiments; the remaining experiments were performed with 0.06 N/m cantilevers (Digital Instruments), with no noticeable differences in the results obtained, according to the cantilever origin. Verifications of the spring constants of the cantilever by the resonance frequency method (Cleveland et al., 1993) gave a value not statistically different from the manufacturer's value for Park Scientific Instruments cantilevers. On the other hand, we found a mean spring constant of 0.03 nN/m for the Digital cantilevers. For each tip used, the sensitivity of the response was determined from force versus distance curves (force curves) on glass coverslips. Force curves of cells (0.9–1.5 Hz) were taken in the same liquid, changing neither the tip nor the position of the laser beam on the cantilever. Contact mode imaging forces were generally adjusted (with no *xy* scanning) to less than 100 pN before the cells were scanned. The slope of the force versus distance curves after contact was adjusted by moving the tip position step by step. Successful imaging of cells was regularly obtained once the force curve acquired a typical curvilinear shape (see, for instance, Fig. 1). According to the drift of the equipment, a 30–90-min equilibration period was generally allowed before the first scanning of cells.

RESULTS

Imaging of CV-1 cells at low magnification

Contact-mode low-force imaging of living CV-1 cells, under phosphate saline buffer supplemented with calcium and glutamine, was achieved on a regular basis. The results of a representative experiment are shown in Fig. 1, where the height and deflection signals of a 80-μm scan of overlaying CV-1 cells and the corresponding force versus distance plot taken just before the scan are presented. The ~60-pN loading force chosen allowed a stable imaging of the cell surface on a large scale. As initially reported by Putman et al. (1992), details of the membrane surface were more easily visualized in the deflection mode than in the height mode. A marked heterogeneity of the surface roughness between

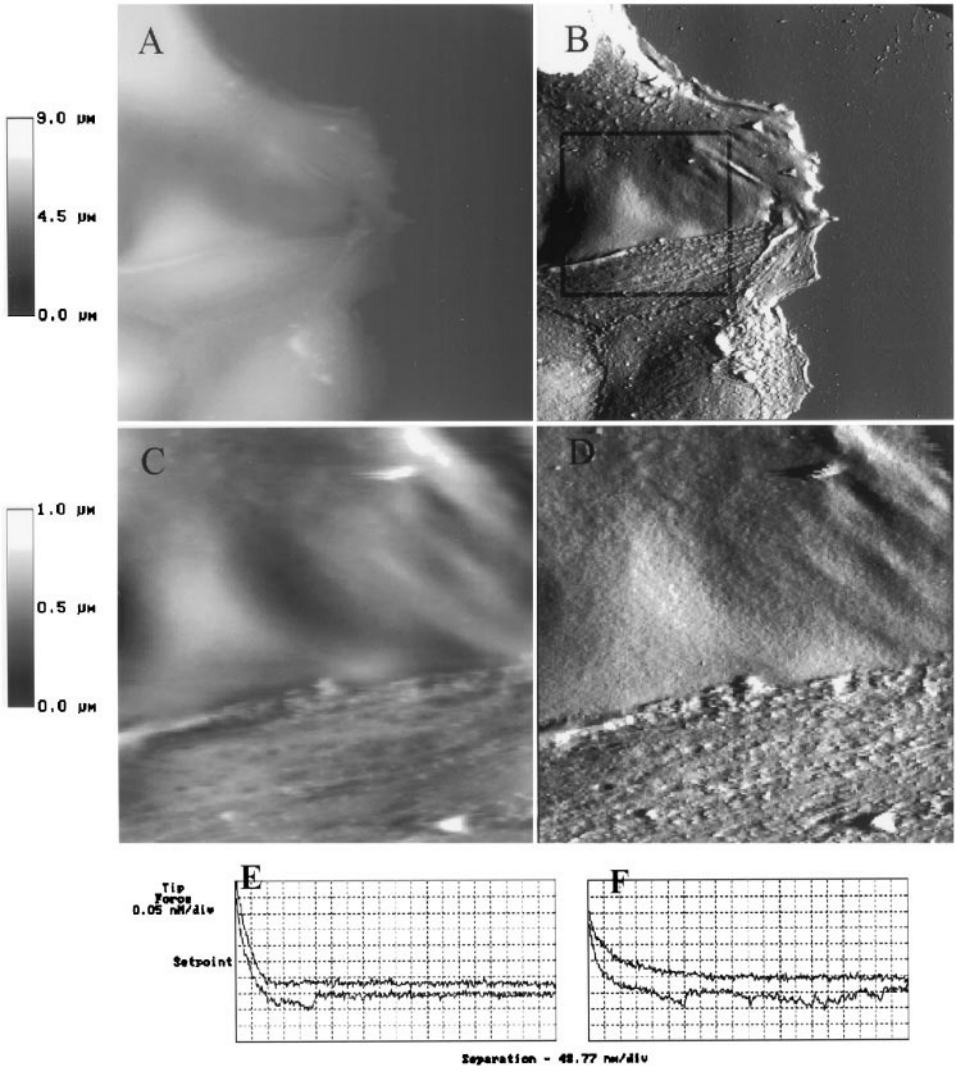

FIGURE 1 Imaging at low-magnification of living CV-1 cells by low-force contact-mode AFM. (*A* (height mode) and *B* (deflection mode; *z* range 5 nm)) 80-μm *xy* scan of a group of cells. Scan rate: 1.2 Hz. (*C* (height mode) and *D* (deflection mode; *z* range 3 nm)) 30-μm *xy* scan of the same group of cells. The box in *B* shows the region chosen for the 30-μm scan. Scan rate: 1.8 Hz. (*E* and *F*) Force versus distance curve corresponding to the imaging of *A–D*, respectively.

adjacent cells, but also for a single cell (see the cell at the upper left corner of the figure), was observed. At this magnification, the images revealed the presence of a few protrusions, some of them ressembling small microvilli, and in some areas of filamentous structures. Most often, reducing the scan size allowed us to further reduce slightly the force needed for imaging. This is illustrated in Fig. 1, *C* and *D*, where the 30-μm scan was obtained with a scanning force of less than 50 pN (Fig. 1 *F*). The images emphasized the topographical heterogeneity of the surface of the CV-1 cells; the relatively smooth surface, with a few protruding, small, round structures observed in the upper part of the figure constrasted with the rougher, more complex aspect of the bottom part, where thin, filamentous structures were discerned. Because the filamentous area corresponded to the edge of one cell overlaying the center area of a different cell, this excluded the possibility that this topographical heterogeneity originated from an artifactual enhanced-contrast effect related to the glass coverslip support. Examination of Fig. 1 *A* showed that, in fact, the smooth and the filamentous areas were at approximately the same height above the glass coverslip. Force and tip position adjustments before scanning constituted an essential procedure for reproducible low-force, contact-mode imaging. Using the default engagement force, the scanning force before any readjustment was generally between 5 and 15 nN, which resulted most of the time in the detachment of the CV-1 cells from the support during the scan (not shown). Successful scanning was obtained when the scanning force was first adjusted to subnanonewton values and the tip was subsequently raised ("tip-up command"), thus working with the piezo in an extended configuration ("quasi-attractive region"). Examination of the force versus distance curves above the center of a cell (Fig. 2), i.e, the "softer" part of the

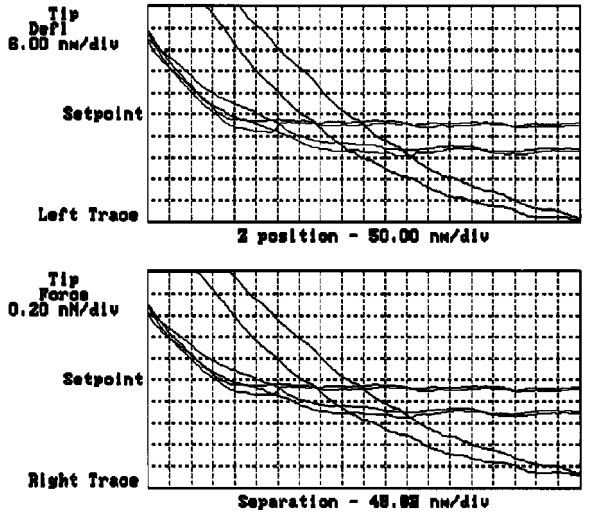

FIGURE 2 Force adjustment before scanning. Representative experiment showing the evolution of cantilever deflection (*upper diagram*) and force (*lower diagram*) versus distance curves obtained at the center of a cell (above the nucleus area), using the procedure described in the text. Cantilever spring constant: 0.01 N/m. *z* scan rate: 1 Hz.

cell, showed that reduction of the scanning force according to the procedure described above had a pronounced effect on the shape of the curves, as well as on the slope of the cantilever deflection after the tip-sample contact. Hysteresis between approaching and retracting curves practically disappeared, and indentation at the set point decreased from 480 nm to 210 nm, and to less than 10 nm when the force was decreased from 800 to 230 and 45 pN, respectively. The effects of a 75-fold variation in the scanning force on the images of the surface of living CV-1 cells are presented in Fig. 3. The same 20-μm cell area was scanned with successive forces of 20, 750, 1500, and 100 pN. Increasing the scanning force from 20 to 750 pN resulted in a marked modification of the surface morphology. The height differences between neighboring, relatively flat areas and protruding structures were accentuated (see sections in Fig. 3) and thin filamentous structures appeared (*thin arrows*). Part of the cell edge damaged during the scan revealed the glass support (*thick arrow*). These modifications were amplified with a 1500-pN scanning force, and other parts of the cell surface seemed to be damaged during imaging. These alterations were at least partly reversed when a low force (100 pN) was applied in the next scan. In particular, the thin filamentous structures, likely corresponding to submembrane cytoskeleton elements, became hardly distinguishable. Marked modifications of the surface were also recorded in the deflection images (not shown). Examination of the sections of a scan line through the image confirmed that the increase in scanning force resulted in an increased contrast between the cytokeleton-supported and the nonsupported zones of the cell surface. On 10-μm scans, even in relatively smooth areas of the cells, the surface appeared highly corrugated when the height range was reduced (Fig. 4). Height differences of a few nanometers between the structures were easily detected, whereas a lateral resolution better than 120 nm was achieved (section in Fig. 4). It is worth noting that, as in many occasions in the present work, force versus distance plots showed the existence of small adhesion forces between the tip and the cell surface when the sample was moved away from the tip (retract trace).

Small scan sizes

The same type of topography was generally observed when small areas were scanned (<5 μm) at low forces (Fig. 5). Some of the protrusions appeared to be arranged along lines. As illustrated by Fig. 6, at this magnification, successive scans of the same area suggested the existence at the cell surface of topographical domains with different dynamics. Thus the big protrusion near the center of the image during the first scan disappeared from the second scan, run 200 s later, whereas the linear structures at the top left of the images were nearly unchanged. Furthermore, the three vertically aligned small pits seen near the center in the first image had practically vanished from the second image, suggesting that the topographical domain located near the

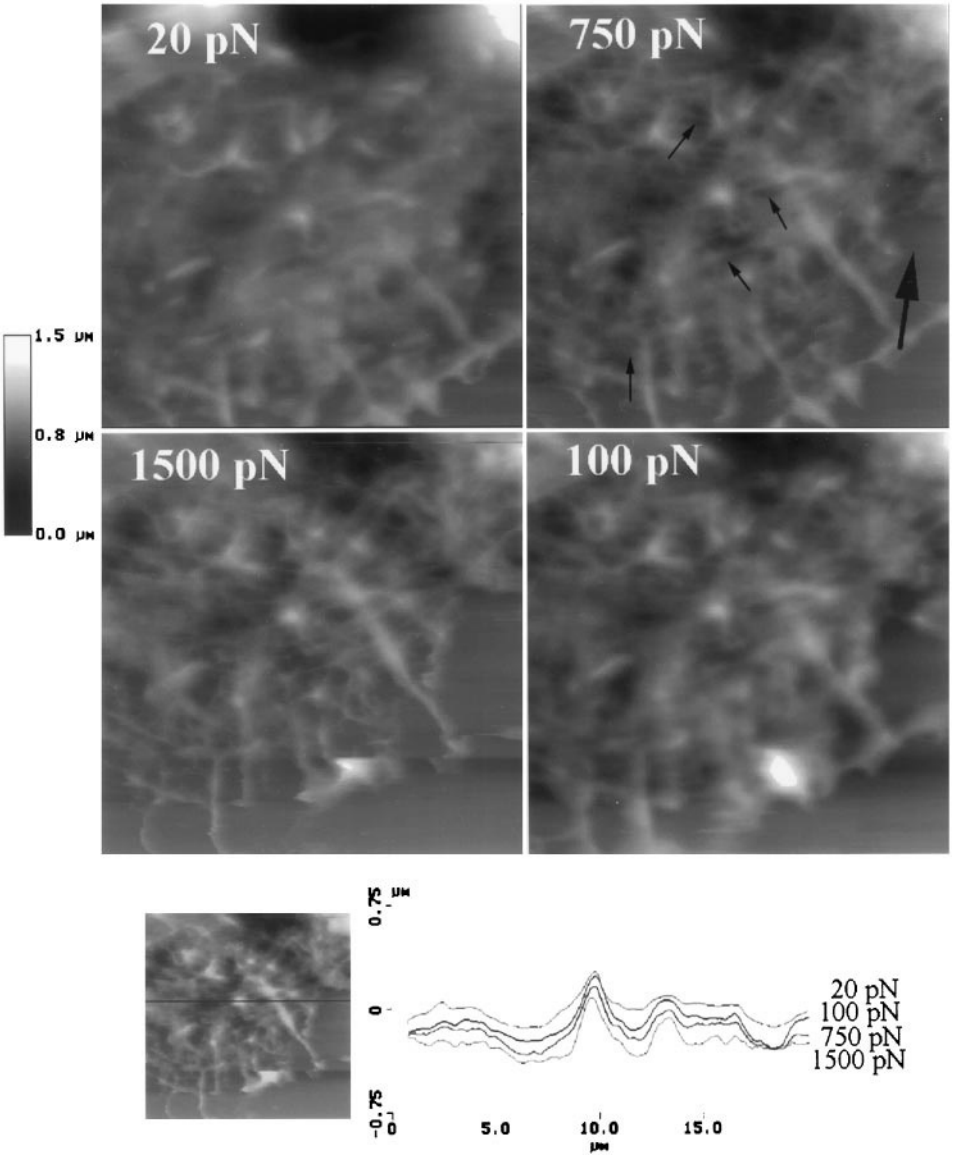

FIGURE 3 Effects of a 75-fold variation in the scanning force on the topography of living CV-1 cells. Height mode. Scan size: 20 μm. Thin arrows: thin filaments. Thick arrow: damaged area. Section shows the height profiles obtained as a function of the scanning force, along a scan line indicated in black. Relative height position of curves was standardized, using the glass support as a reference. Scan rate: 1.2 Hz.

image center was less stable than the one visualized at the top left. Frequently, on 2-μm scans, tiny particles were detectable in part of the image on the computer screen (Fig. 7). Zooming in on these particular zones, which were generally rather flat, 800-1000-nm scans repeatedly revealed structures such as those presented in Fig. 7, *C* and *D*. In these zones, the cell surface appeared to be covered by globular particles of irregular size. On such scans the lateral resolution was regularly better than 20 nm. The *xy* size of the particles was generally between ~10 and 30 nm (Fig. 7 *E*). Occasionally, a slightly better resolution (7–5 nm) was achieved by reducing the scan size, while keeping the force minimal (Fig. 8). Interestingly, the lateral (friction) force images (Fig. 8, *B* and *D*) often showed more details and a better resolution than the height images simultaneously acquired (Fig. 8, *A* and *C*). It is noteworthy that "high-resolution" imaging of the cell surface was only obtained when scanning forces were kept at the limit of the force feedback regulation of the AFM. Finally, care was taken to scan a much large zone after each small scan to ensure that the "high-resolution" scanned area effectively corresponded to a part of the cell surface and not to the support.

DISCUSSION

The present experiments demonstrate that in the contact mode, scanning forces as low as 20–50 pN provided stable imaging of the surface of living CV-1 cells by AFM. With these scanning forces, which were 50–1000 times lower than those commonly used for AFM cell imaging, the tridimensional topography of the CV-1 cell surface, at low magnification, appeared heterogeneous, with zones of different roughness. A lateral resolution significantly better than that of the light microscope was already obtained from 10–30-μm scans. Reducing the scan size suggested the

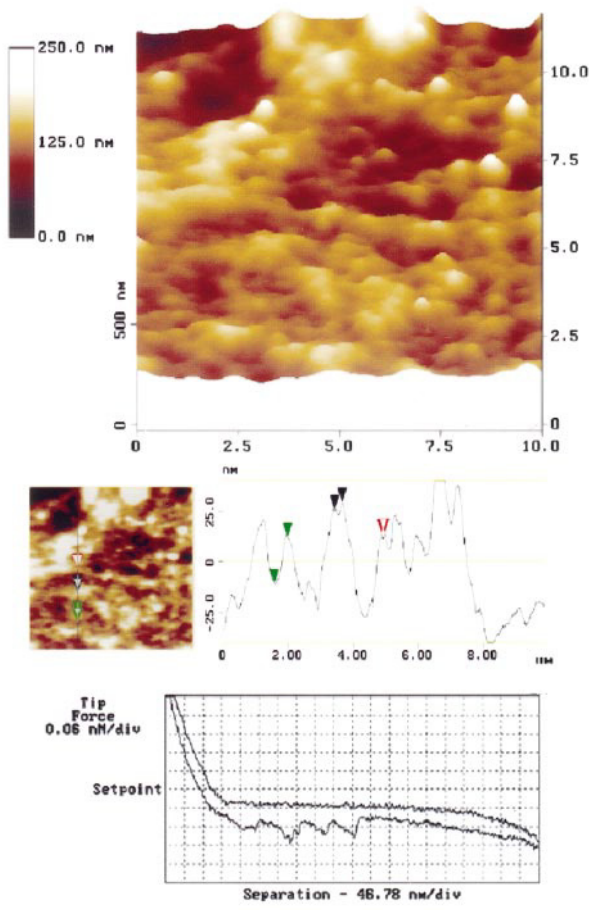

FIGURE 4 Ten-micron scan of the surface of CV-1 cells and corresponding section and force versus distance curve. Horizontal distances between the pairs of green, black, and red arrows were 293, 195, and 118 nm, respectively. Scan rate: 2 Hz.

existence at the cell surface of topographical domains with different lifetimes. Under favorable circumstances, the best lateral resolution achieved for the living CV-1 cells was ~7–5 nm. At this resolution, the surfaces probed appeared to be constituted of, or covered by, tightly packed globular particles of various sizes.

Low-force imaging

The scanning forces used for imaging of intact cells are generally between 1–5 nN and 30 nN (Henderson et al., 1992; Oberleithner et al., 1993; Hoh and Schoenenberger, 1994; Putman et al., 1994; Haydon et al., 1996; Radmacher et al., 1996). Different factors were involved in the successful imaging of intact cells at much lower forces: first, the use of cantilevers with 0.01–0.03 N/m spring constants, which allowed a precise adjustment of the imaging force in the low-force regime before scanning, and consequently, a 30–90-min equilibration period, required for "stabilization" of the cantilever position. Such a stabilization period, after which a reasonable drift (~0.2 nm/min) that could be corrected manually during the scan still occurred, likely depended on the thermal equilibration between the cantilever, heated by the laser spot, and the surrounding liquid medium (Kipp et al., 1995). One has to remember that at 50-pN loading force, the signal-to-noise ratio is still ~60 and ~20 for 0.01 and 0.035 N/m cantilevers, respectively (Shao et al., 1996). The second important maneuver before scanning was to adjust the tip-sample distance to get the best correspondence between the approach and retract traces in the force plot. This was generally obtained with the piezo working close to the maximum extended position ("quasi-attractive region"). This maneuver modified both the shape of the curves and the slope of the cantilever deflection after the tip-sample contact, and this was more pronounced for the cell center than for the cell periphery. In fact, using forces of ≤50 pN, comparison of the forces curves obtained on glass and on the cell surface showed that "indentation" was very limited, not only at the cell edges, but also at the cell center (see Fig. 2). Considering the most unfavorable situation, that is, that the surface negative charge of the mica is as large as that of a biological membrane, which is notably an underestimate (Sherbet, 1978; Müller and Engel, 1997) for determining the onset of the cell surface-tip contact, the indentation at the center of the cell for 45 pN was below 10 nm, leading to a Young's modulus of ~400 kPa, assuming a Poisson ratio of 0.5 and a 30° opening angle for the tip (Radmacher et al., 1996). Estimates of the Young's modulus at the cell periphery, for instance, from the force versus distance curve corresponding to Fig. 5, also gave values of ~400 kPa, i.e., not different from that obtained for the cell center. The observation that, at low forces, the Young's modulus was approximately constant over the cell

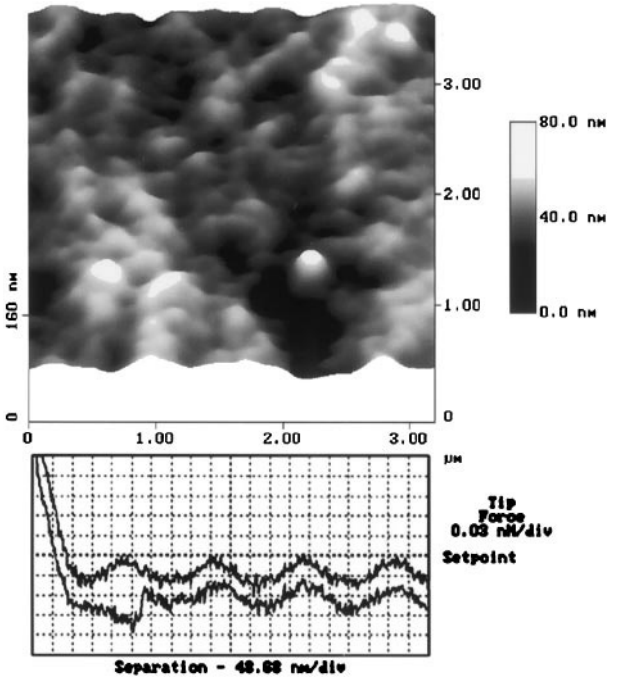

FIGURE 5 Three-micron scan of the surface of CV-1 cells and corresponding force versus distance curve. Scan rate: 2 Hz.

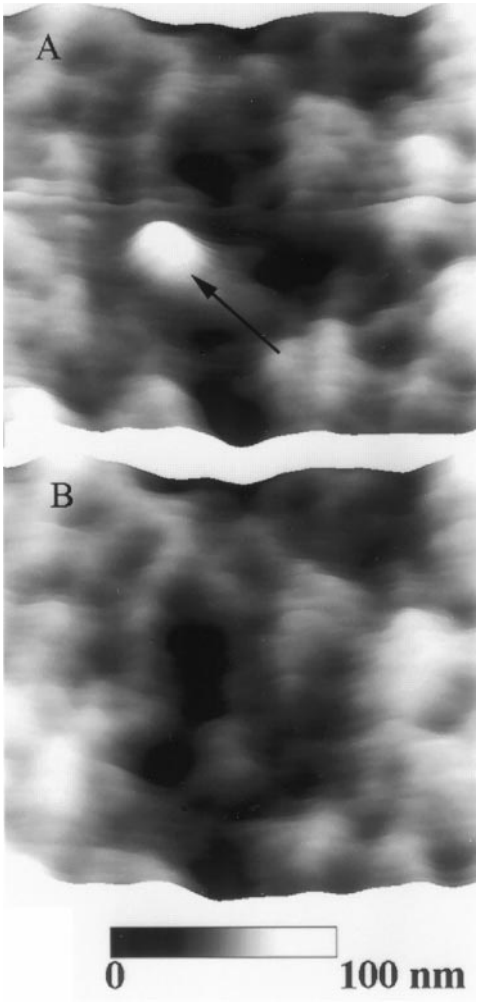

FIGURE 6 Topographical modification between successive scans. Scan size: 2 μm. Scan force: 80 pN. Scan rate: 2.5 Hz.

surface is in agreement with the data obtained, albeit at higher forces (150–300 pN) and under nonimaging conditions, by Radmacher et al., (1996). Accordingly, the use of low-force scans and the Young's modulus values estimated for CV-1 cells could account for the resolution better than 7–5 nm at the surface of a living cell (Weisenhorn et al., 1993). Examination of force versus distance plots also revealed, on many occasions, the presence of small adhesion forces when the sample was moved away from the tip (retract trace). Although the origin of these small adhesion forces cannot be ascertained, they might be related to the transfer of tiny membrane components to the probe (Schaus and Henderson, 1997). By creating small protrusions at the end of the tip, this might also contribute to improving the resolution of imaging. The third parameter involved in successful low-force imaging concerned the cell type used. Using the same procedure, low-force imaging was also obtained for living Madin-Darby canine kidney (MDCK) cells, allowing the imaging of tightly packed microvilli (not shown), but so far has failed when applied to an other cell line, the 3T3 fibroblast cells. This strongly suggested that the chemical/mechanical properties of the cell surfaces vary markedly between cell types, which thus may or may not render low-force imaging possible. It is noteworthy that, even when using cantilevers with the lowest spring constants, starting a scan just after the automatic approach and the detection of the tip-sample contact by the AFM (default engagement force), i.e., with no real force adjustment, often resulted in cell damage. In fact, with CV-1 cells, cell damage could even occur for forces below 1 nN (see Fig. 3).

Topography of the CV-1 cell surface

Examination of CV-1 cells at low magnification revealed a marked heterogeneity of the surface topography, with zones enriched in thin filamentous structures coexisting with smoother zones. This heterogeneity, best visualized by the error signal images, was also clearly visible in the height mode images. Plasma membrane deformation under the AFM tip or tip penetration through the cell membrane has been proposed to explain the visualization by AFM of the thin filamentous structures, which correspond to elements of the submembrane cytoskeleton, at the surface of cells (Henderson et al., 1992). Recent experiments, however, rule out the tip penetration hypothesis (Haydon et al., 1996; Schaus and Henderson, 1997). The observation that comparable images of a cell surface are obtained using scanning forces as low as 20–30 pN, with indentations smaller than 10 nm, raises questions about the current interpretation of submembrane cytoskeleton visualization. An alternative to the "draping model," in which the vertical applied force from the AFM tip causes the membrane to "drape" over rigid subcellular structures during imaging (Henderson et al., 1992), could be that, under normal conditions the plasma membrane, in places, lies on submembrane structures. Tightness of the coupling between submembrane structures and the plasma membrane would vary locally as a function of the cytoskeleton organization and its anchoring to membrane proteins, as well as a function of local chemical/osmotic gradients. Such a hypothesis is consistent with the observation that, most often, "filamentous" zones coexist with "smooth" zones at the cell surface. The observation that such filamentous zones can be imaged from cell extensions partially covering the center domain of other cells (Fig. 1) strongly argues against the view that the filamentous aspect is only a consequence of the fact that the cell edge, containing less cytoplasm, sits as a thin layer on the hard surface of the glass support, thus allowing a better resolution of the submembrane structures. It is also consistent with the notion of domains, whose existence would depend, at least partly, on cytoskeleton-membrane protein interactions in plasma membranes (Kusumi and Sako, 1996). Finally, it also provides an explanation for the images presented in Fig. 3, where the scanning force was varied from 20 pN to 1.5 nN. Long, tubular structures that abut the cell border, as well as large protruding structures, were observed at 20 pN. The height of these protruding

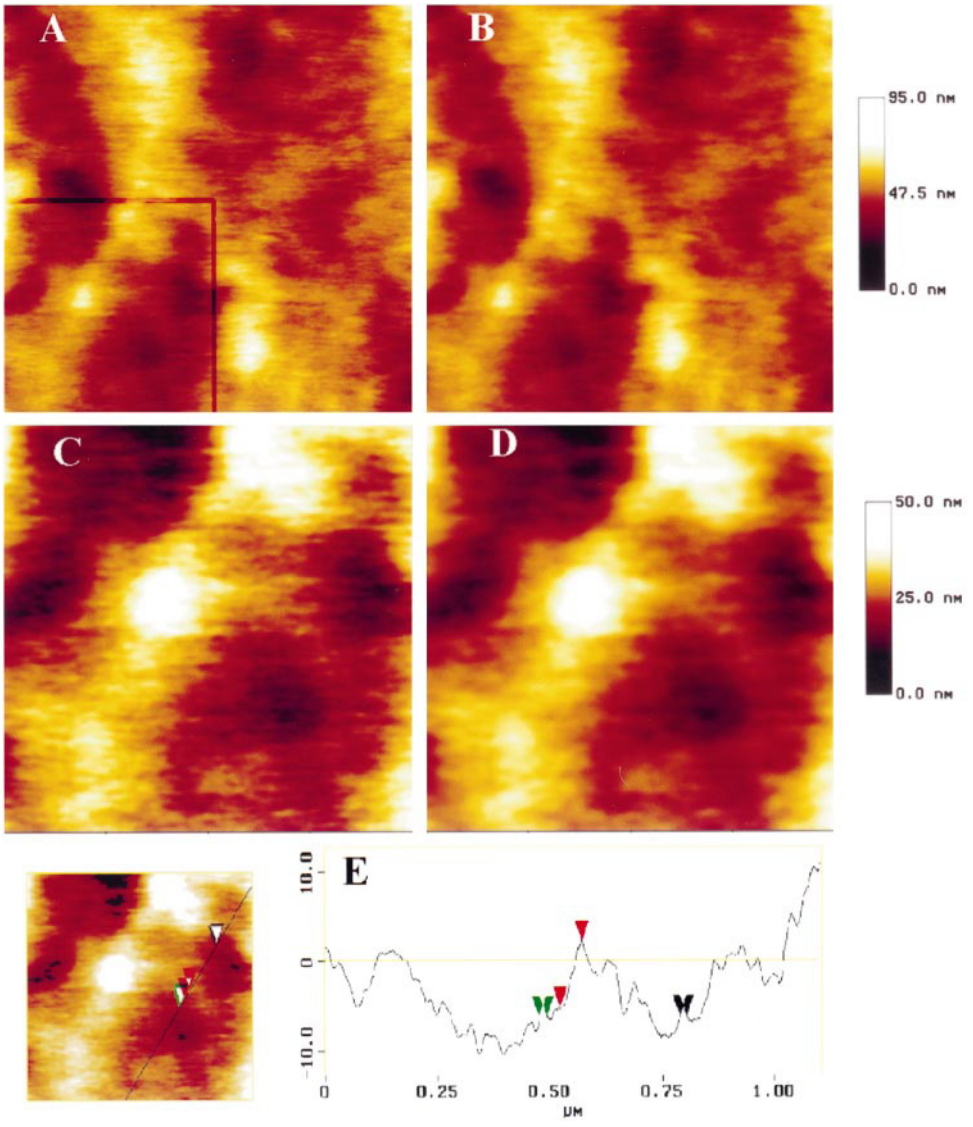

FIGURE 7 High-magnification imaging of the cell surface at low force. (*A*) Two-micron scan of the surface of living CV-1 cells (height mode, raw image). The presence of tiny particles is visible on the lower left corner of the image. Scan force: 60 pN; scan rate: 1.2 Hz. (*C*) One-micron electronic zoom of the lower left corner, identified by a box, of *A*. *B* and *D* correspond to *A* and *C*, respectively, after low-pass filtering. (*E*) Section analysis of *C*. Horizontal distances between the pairs of green, red, and black arrows were 17.6, 49.0, and 15.7 nm, respectively. The vertical distance between the pair of red arrows was 7.3 nm.

structures indicates that they correspond to submembrane structures (intracellular organelles?) recovered by the plasma membrane, rather than to extensions of the plasma membrane itself. In addition to these structures, increasing the scanning force to 750 pN revealed the existence of transversal long filamentous structures likely corresponding to actin filaments, which in this region of the cell were localized deeper below the cell surface. The phenomenom was amplified at 1.5 nN, where marked cell damage occurred. This damage was not irreversible, as shown by the next scan at 100 pN, in which most of the thin filaments previously observed at high scanning force again became indiscernible. These images extend to the low-force work done by Radmacher et al. (1996), who, starting at 0.4 nN, reconstructed from single topographical lines the constant force topographs from a human platelet.

Decreasing the scan size to 10 μm and keeping low scanning forces reinforced the view that cell surface topography was markedly dependent on submembrane structural organization. Thus structures that protrude 80–100 nm above the surface likely represented extensions of the plasma membrane supported by internal structures. It has to be mentioned that, with such scan sizes, the lateral resolution (~100 nm) was already better than the resolution of an optical microscope. This was further confirmed with smaller scan sizes, which also allowed us to observe local submicron rearrangements of the cell surface between two successive scans. Frequently, zones of tiny packed particles were observed in 2-μm raw images. These particles, ~10–30 nm *xy* size, protuded up to ~8 nm above the surface and were better visualized after low-pass filtering. These observations confirm those made by a few groups of investigators working on different cell types (Butt et al., 1990; Hörber et al., 1992; Le Grimellec et al., 1994), who reported that, when accessible to high resolution, the cell surface appears to be constituted of particles that occupy most of the membrane surface. Because, at this time, less attention was paid to the fine control of scanning forces, it is likely that these high-resolution images were the result of very low force, involuntary scans. It is noteworthy that a

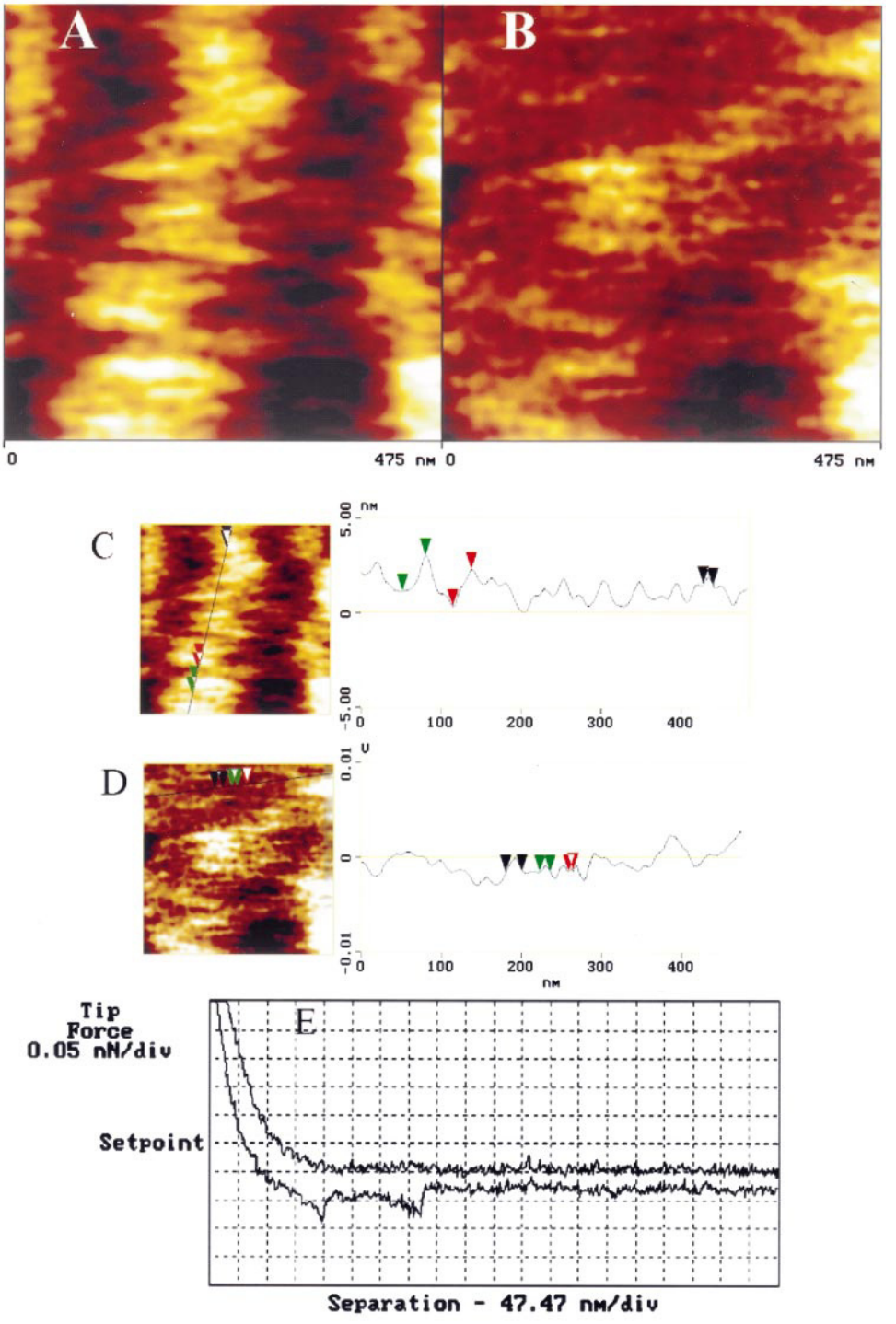

FIGURE 8 Submicron scan of the surface of living CV-1 cells. Scan size: 475 nm. Scan rate: 2 Hz. (*A*) Height image (low-pass filtered). *z* range: 10 nm. (*B*) Friction image (low-pass filtered). *z* range: 0.025 V. (*C*) Section analysis of *A*. Vertical distances between the pairs of green and red arrows were both 1.9 nm. Horizontal distance between the pair of black arrows: 7.2 nm. (*D*) Section analysis of *B*. Horizontal distances between the pairs of green, red, and black arrows were 7.4, 5.6, and 14.8 nm, respectively. (*E*) Corresponding force versus distance curve.

similar organization was observed for supported isolated plasma membranes examined under liquid (Le Grimellec et al., 1995; Lärmer et al., 1997). Such particles or globular structures are redistributed upon concanavalin A addition at the surface of red blood cells (Hörber et al., 1992), are digested by protease treatment of the surface of MDCK cells (Le Grimellec et al., 1994), and are still present on the cytoplasmic leaflet of the plasma membrane of MDCK cells after ethanol dehydration (Le Grimellec et al., 1995), a procedure that extracts a large fraction of membrane lipids. This strongly suggests that they correspond to membrane proteins or to protein-lipid complexes. In contrast to the data obtained on MDCK cells (Le Grimellec et al., 1994), no enzymatic treatment was required to gain access to the membrane surface. This suggests that CV-1 cells have a glycocalix less abundant than that of MDCK cells. Likely, the fact that the small particles were visualized only from particular zones is related to a nonuniform distribution of the glycocalix over the cell surface. On some occasions, the lateral resolution was improved to 5–7 nm by submicron

scans. The images thus obtained confirmed the size heterogeneity of the membrane particles. Lateral force (friction) images also confirmed the existence of the particles, often offering a better definition than the height images acquired simultaneously.

This work was supported by grants from La Fondation pour la Recherche Médicale, l'Association pour la Recherche sur le Cancer, la Région Languedoc-Roussillon, and l'Université Montpellier I. VV was supported by a scholarship grant from the Région Languedoc-Roussillon.

REFERENCES

Butt, H. J., E. K. Wolff, S. A. C. Gould, B. Dixon Northern, C. M. Peterson, and P. K. Hansma. 1990. Imaging cells with the atomic force microscope. *J. Struct. Biol.* 105:54–61.

Cleveland, J. P., S. Manne, D. Bocek, and P. K. Hansma. 1993. A nondestructive method for determining the spring constant of cantilevers for scanning force microscopy. *Rev. Sci. Instrum.* 64:403–405.

Fritz, M., M. Radmacher, and H. E. Gaub. 1994. Granula motion and membrane spreading during activation of human platelets imaged by atomic force microscopy. *Biophys. J.* 66:1328–1334.

Häberle, W., J. K. H. Hörber, and G. Binnig. 1991. Force microscopy on living cells. *J. Vac. Sci. Technol. B.* 9:1210–1213.

Haydon, P. G., R. Lartius, V. Parpura, and S. P. Marchese-Ragona. 1996. Membrane deformation of living glial cells using atomic force microscopy. *J. Microsc.* 182:114–120.

Henderson, E.. 1994. Imaging of living cells by atomic force microscopy. *Prog. Surf. Sci.* 46:39–60.

Henderson, E., P. G. Haydon, and D. S. Sakaguchi. 1992. Actin filaments dynamics in living glial cells imaged by atomic force microscopy. *Science.* 257:1944–1946.

Hoh, J. H., and C-A. Schoenenberger. 1994. Surface morphology and mechanical properties of MDCK monolayers by atomic force microscopy. *J. Cell Sci.* 107:1105–1114.

Hörber, J. K. H., W. Häberle, F. Ohnesorge, G. Binnig, H. G. Liebich, C. P. Czerny, H. Mahnel, and A. Mayr. 1992. Investigation of living cells in the nanometer regime with the scanning force microscope. *Scanning Microsc.* 6:919–930.

Ito, E., T. Takahashi, K. Hama, T. Yoshioka, W. Mizutani, H. Shimizu, and M. Ono. 1991. An approach to imaging of living cell surface topography by scanning tunneling microscopy. *Biochem. Biophys. Res. Commun.* 177:636–643.

Kipp, S., R. Lacmann, and M. A. Schneeweiss. 1995. Problems in temperature control performing in situ investigations with the scanning force microscope. *Ultramicroscopy.* 57:333–335.

Kusumi, A., and Y. Sako. 1996. Cell surface organization by the membrane skeleton. *Curr. Opin. Cell Biol.* 8:566–574.

Lärmer, J., S. W. Schneider, T. Danker, A. Schwab, and H. Oberleitner. 1997. Imaging excised apical plasma membrane patches of MDCK cells in physiological conditions with atomic force microscopy. *Pflügers Arch. Eur. J. Physiol.* 434:254–260.

Le Grimellec, C., E. Lesniewska, C. Cachia, J. P. Schreiber, F. de Fornel, and J. P. Goudonnet. 1994. Imaging the membrane surface of MDCK cells by atomic force microscopy. *Biophys. J.* 67:36–41.

Le Grimellec, C., E. Lesniewska, M-C. Giocondi, C. Cachia, J. P. Schreiber, and J. P. Goudonnet. 1995. Imaging of the cytoplasmic leaflet of the plasma membrane by atomic force microscopy. *Scanning Microsc.* 9:401–411.

Le Grimellec, C., E. Lesniewska, M-C. Giocondi, E. Finot, and J. P. Goudonnet. 1997. Simultaneous imaging of the surface and the submembraneous cytoskeleton in living cells by tapping mode atomic force microscopy. *C. R. Acad. Sci. Paris.* 320:637–643.

Müller, D. J., G. Büldt, and A. Engel. 1995a. Force-induced conformational change of bacteriorhodopsin. *J. Mol. Biol.* 249:239–243.

Müller, D. J., and A. Engel. 1997. The height of biomolecules measured with the atomic force microscope depends on electrostatic interactions. *Biophys. J.* 73:1633–1644.

Müller, D. J., F. A. Schabert, G. Büldt, and A. Engel. 1995b. Imaging purple membrane in aqueous solution at sub-nanometer resolution by atomic force microscopy. *Biophys. J.* 68:1681–1686.

Oberleithner, H., G. Giebisch, and J. Geibel. 1993. Imaging the lamellipodium of migrating epithelial cells in vivo by atomic force microscopy. *Pflügers Arch.* 425:506–510.

Putman, C. A., K. O. van der Werlf, B. G. de Grooth, N. F. van Hulst, and J. Greve. 1994. Viscoelasticity of living cells allows high resolution imaging by tapping mode atomic force microscopy. *Biophys. J.* 67: 1749–1753.

Putman, C. A., K. O. van der Werlf, B. G. de Grooth, N. F. van Hulst, J. Greve, and P. K. Hansma. 1992. A new imaging mode in atomic force microscopy based on the error signal. *Proc. Soc. Photo-Opt. Instrum. Eng.* 1639:198–204.

Radmacher, M. 1997. Measuring the elastic properties of biological samples with the AFM. *I.E.E. Eng. Med. Biol.* March/April:47–57.

Radmacher, M., M. Fritz, and P. K. Hansma. 1995. Imaging soft samples with the atomic force microscope: gelatin in water and propanol. *Biophys. J.* 69:264–270.

Radmacher, M., M. Fritz, C. M. Kacher, J. P. Cleveland, and P. K. Hansma. 1996. Measuring the viscoelastic properties of human platelets with the atomic force microscope. *Biophys. J.* 70:556–567.

Radmacher, M., R. W. Tillmann, M. Fritz, and H. E. Gaub. 1992. From molecules to cells: imaging soft samples with the atomic force microscope. *Science.* 257:1900–1905.

Ruppersberg, J. P., J. K. H. Hörber, C. Gerber, and G. Binnig. 1989. Imaging of cell membraneous and cytoskeletal structures with a scanning tunneling microscope. *FEBS Lett.* 257:460–464.

Schaus, S. S., and E. R. Henderson. 1997. Cell viability and probe-cell membrane interactions of XR1 glial cells imaged by atomic force microscopy. *Biophys. J.* 73:1205–1214.

Shao, Z., J. Mou, D. M. Czajkowsky, J. Yang, and J-Y. Yuan. 1996. Biological atomic force microscopy: what is achieved and what is needed. *Adv. Phys.* 45:1–86.

Sherbet, G. V. 1978. The Biophysical Characterisation of the Cell Surface. Academic Press, London.

Weisenhorn, A. L., M. Khorsandi, S. Kasas, V. Gotzos, and H-J. Butt. 1993. Deformation and height anomaly of soft surfaces studied with an AFM. *Nanotechnology.* 4:106–113.